Supplementary Information

Surface-Dominated Transport and Enhanced Thermoelectric Figure of Merit in Topological Insulator $Bi_{1.5}Sb_{0.5}Te_{1.7}Se_{1.3}$

Te-Chih Hsiung,[a,b,c*] Chung-Yu Mou,[d] Ting-Kuo Lee,[a,c] and Yang-Yuan Chen[c,e*]

[a] Department of Physics, National Taiwan University, Taipei 106, Taiwan.
[b] Nano Science and Technology Program, Taiwan International Graduate Program, Academia Sinica, Taipei, Taiwan and National Taiwan University, Taipei, Taiwan
[c]. Institute of Physics, Academia Sinica, Taipei 11529, Taiwan.
[d] Department of Physics, National Tsing Hua University, Hsinchu 30013, Taiwan
[e] Graduate Institute of Applied Physics, National Chengchi University, Taipei 116, Taiwan

Corresponding Authors

* E-mail: cheny2@phys.sinica.edu.tw; techi@phys.sinica.edu.tw

A. Thermal conductivity measurement using the 3ω method

The NW thermal conductivity was measured using the self-heating 3ω method [S1,S2]. By applying an AC current $I_0 \sin \omega t$ to the suspended NW, the NW serves as a heater and temperature sensor and produces a temperature fluctuation at 2ω. This further induces a voltage fluctuation at 3ω, $V_{3\omega}$, across the voltage contact. The term $V_{3\omega}$ can be expressed as [S1,S2] $V_{3\omega} = \frac{4 I^3 L R R'}{\pi^4 k S \sqrt{1+(2\omega\gamma)^2}}$, where I is the rms value of $I_0 \sin \omega t$, R and R' are the resistance and the derivative of resistance, respectively, with respect to temperature, κ is the thermal conductivity of NW, L is the length of the NW between the voltage contacts, S is its cross-section area, and γ is the characteristic thermal time constant. In the low-frequency limit ($\omega\gamma \rightarrow 0$), $V_{3\omega}$ can be expressed as $V_{3\omega} = \frac{4 I^3 L R R'}{\pi^4 k S}$. Figure S1a shows the $V_{3\omega}$ signal following the cubic dependence of I_0. Figure S1b shows the frequency response to the $V_{3\omega}$ signal. The thermal conductivity can be derived by fitting the $V_{3\omega}$ signal to I_0 at a certain temperature, as shown in Figure S2.

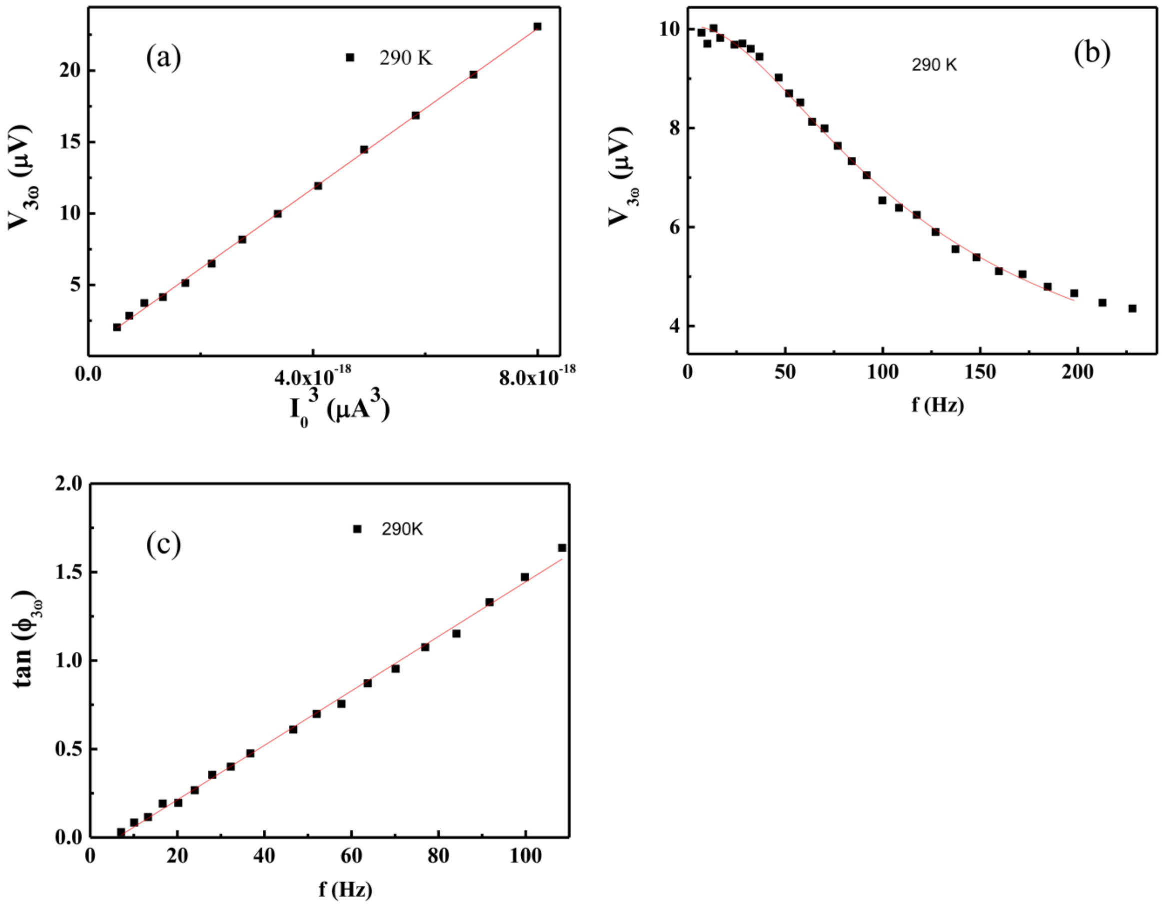

Figure S1. *3ω* signals of individual BSTS NW4. (a) *3ω* voltage as function of the applied current. The solid line shows the predicted relation of $V_{3\omega}$ and I. (b) The $V_{3\omega}$ versus frequency plot. (c) The frequency dependence of the phase shift of *3ω* voltage.

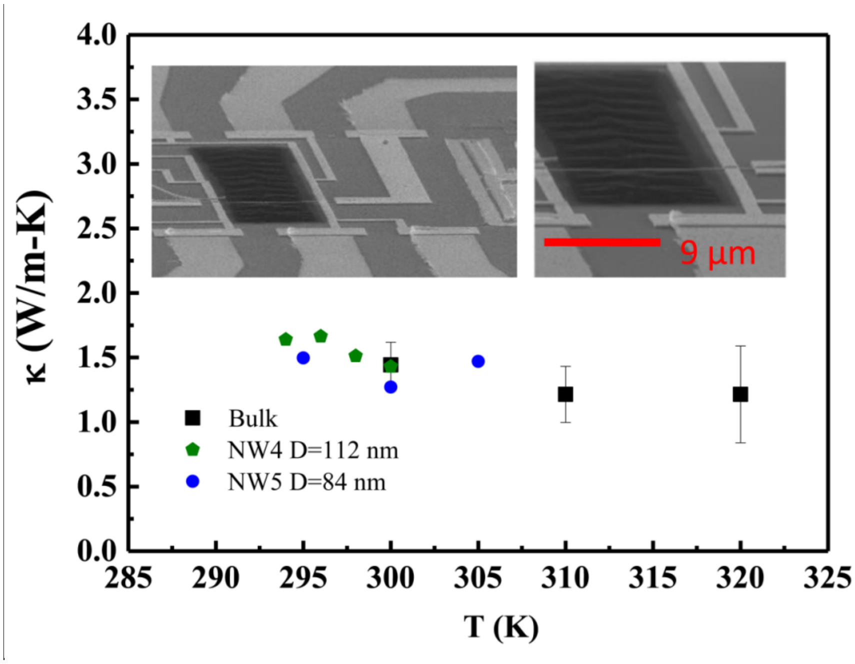

Figure S2. The temperature dependence of the thermal conductivity of the BSTS specimens. The insets show the SEM images of suspended NWs.

BSTS	Diameter (nm)	S (μV/K)	ρ (μΩ-m)	PF (10^{-4} W/m-K^2)	κ (W/m-K)	ZT	Reference
NW 1	180	-259	41.9	16.11	1.33*	0.36	This work
NW 2	230	-228	55.4	9.38	1.33*	0.21	This work
Bulk		-235.8	399.5	1.33	1.4	0.028	This work
BSTS	Bulk		1400				S3
BSTS	Bulk		500				S4
Nanoflake	596 nm thick		500				S5

Table 1 Summary of TE parameters for BSTS NWs and bulk materials, measured at 300 K.

B. SEM image of the measurement device for NW2

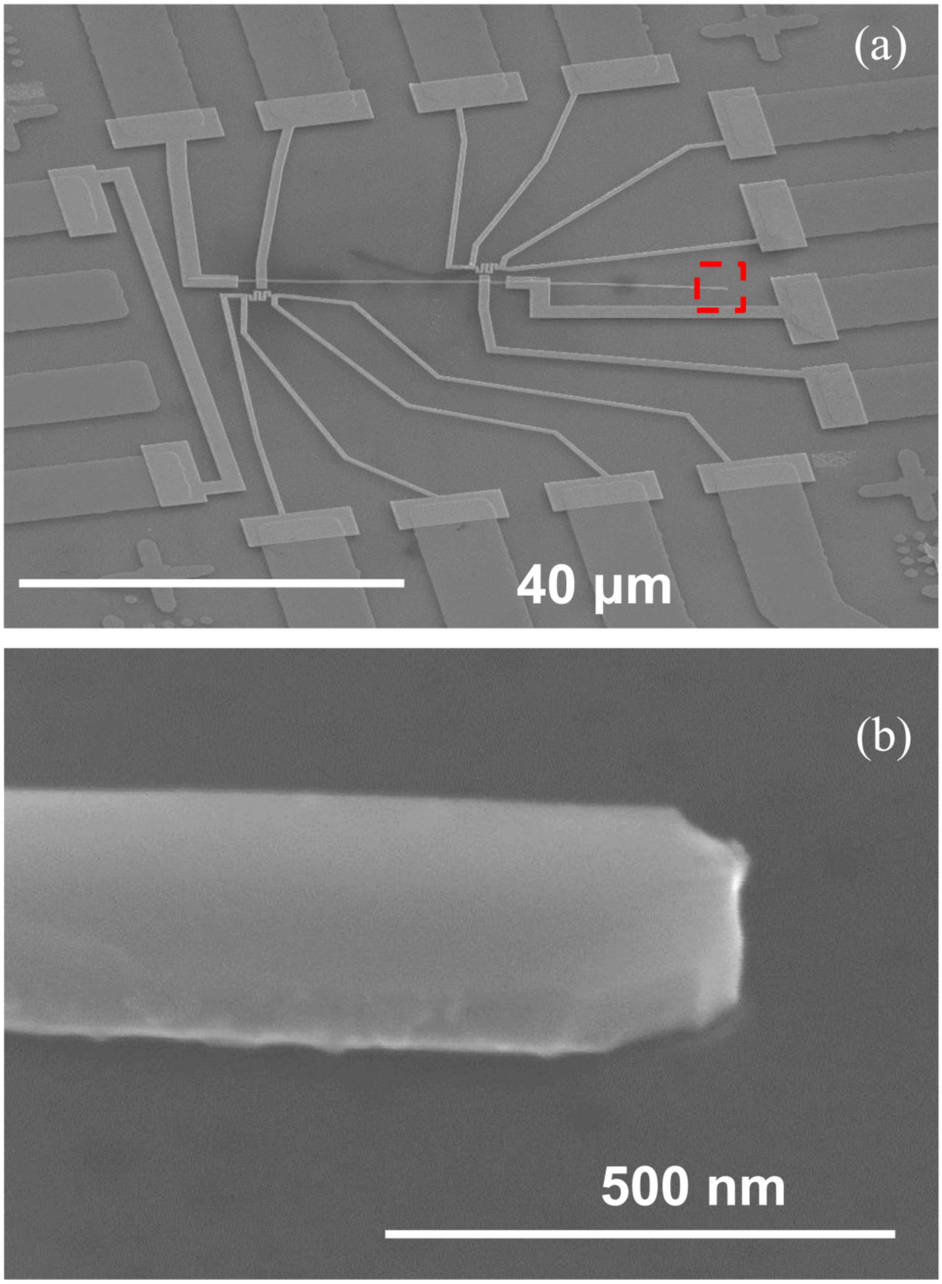

Figure S3. (a) A SEM image of the device for Seebeck coefficient and electrical conductivity measurements. (b) Cross-section SEM image of the dashed line area of Fig. S3(a).

C. Estimating mobility from magnetoresistance

Figure S3 shows the comparison between MR mobility, Hall measurements, and the linear part of the slope of MR. The measured Hall carrier mobility and extraction of MR mobility [S6,S7] are shown in the right scale. By adjusting the left scale of dMR/dH, the corresponding carrier mobility values are obtained and their temperature dependence is consistent with each other.

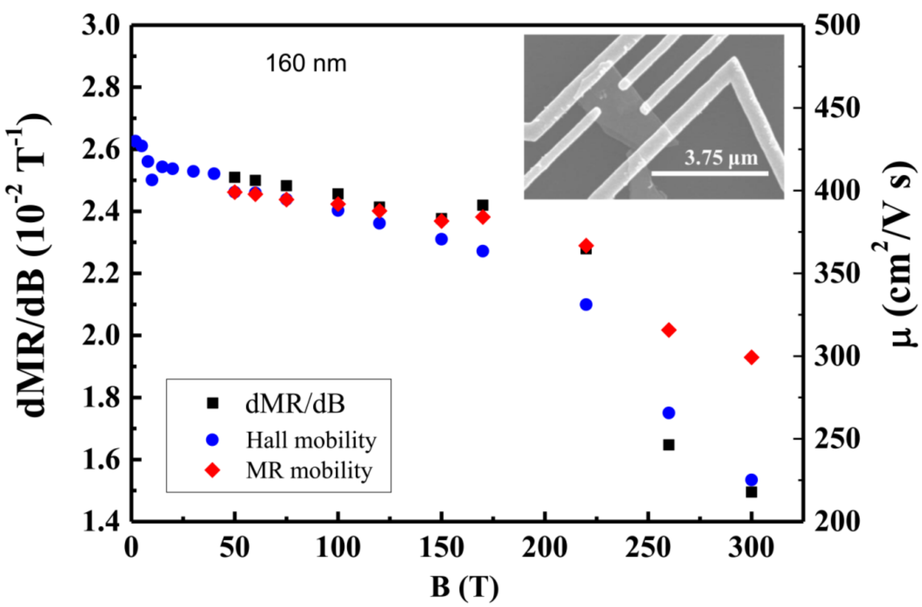

Figure S4. Temperature dependence of mobility of BSTS nanolfake. The inset shows the SEM image of the measured BSTS nanoflake 160 nm in thickness. The measured Hall carrier mobility and extraction of MR mobility are shown in the right scale. The left scale, dMR/dH, is the slop of LMR.

References

S1. Lu, L.; Yi, W.; Zhang, D. L. *Rev. Sci. Instrum.* **2001**, 72, 2996−3003.

S2 Li, G.; Liang, D.; Qiu, R. L. J.; Gao, X. P. A. *Appl. Phys. Lett.* **2013**, 102, 043104.

S3. Ren, Z.; Taskin, A. A.; Sasaki, S.; Segawa, K.; Ando, Y. *Phys. Rev. B* 2011, 84, 165311.

S4. Taskin, A. A.; Ren, Z.; Sasaki, S.; Segawa, K.; Ando, Y. *Phys. Rev. Lett.* **2011**, 107, 016801.

S5. Xia, B.; Ren, P.; Sulaev, A.; Liu, P.; Shen, S.-Q.; Wang, L. *Phys. Rev. B* **2013**, 87, 085442.

S6. Thevenod, L.; Cassé, M.; Desrat, W.; Mouis, M.; Reimbold, G.; Maude, D. K.; Boulanger, F. *Appl. Phys. Lett.* **2007**, 90, 152111.

S7. Meziani, Y. M.; Lusakowski, J.; Knap, W.; Dyakonova, N.; Teppe, F.; Romanjek, K.; Ferrier, M.; Clerc, R.; Ghibaudo, G.; Boeuf, F.; Skotnicki, T. *J. Appl. Phys.* **2004**, 96, 5761-5765.